Eur. Phys. J. B (2019) 92: 131
https://doi.org/10.1140/epjb/e2019-90501-8

THE EUROPEAN PHYSICAL JOURNAL B

Regular Article

Effect of boundary scattering on spin-hall effect

Shishir K. Pandey[1,a,b] and Tribhuvan P. Pareek[2,3]

[1] Department of Physics, National Taiwan University, No. 1, Sec. 4, Roosevelt Rd., Taipei 10617, Taiwan
[2] Harish-Chandra Research Institute, Chhatnag Road, Jhunsi, Allahabad 211019 India
[3] Homi Bhaha National Institute, Anushaktinagar Mumbai, Maharashtra 400094, India

Received 10 August 2018 / Received in final form 4 April 2019
Published online 19 June 2019
© EDP Sciences / Società Italiana di Fisica / Springer-Verlag GmbH Germany, part of Springer Nature, 2019

Abstract. The spin dependent reflection in quasi-two-dimensional electron gas from an impenetrable barrier in presence of Rashba and Dresselhaus spin-orbit coupling is analysed in detail. It is shown that the due to spin-orbit effects the reflected beam split in two beams gives rise to multiple reflection analogous to phenomenon birefringence. The interplay between Rashba and Dresselhaus spin orbit coupling gives rise to anisotropy in Fermi energy surface and a non-zero net spin-polarized current oscillating with two frequencies for all the values of incident angle except at 45° when averaged over all components of reflected beam. It is also shown that in over critical region,all the three polarization components as well as net polarization has non-zero values and are exponentially decaying as distance from the barrier increases which in turns spin-accumulation near the barrier is an important consequence of spin-hall effect.

1 Introduction

The manipulation and coherent control of electronic spin degree of freedom has emerged as an important area of research in recent years. It in turn requires the ability to generate, inject and control spin polarized charge current – an example of that is Datta–Das spin-transistor [1], where a semiconductor is sandwiched between two Ferromagnetic contacts. The injection and detection of spin polarized current is achieved by using Ferromagnetic contacts in which spin is easier to manipulate because it behaves as a collective degree of freedom. In the semiconductor region, coherent control of spin polarized current is done using the band structure spin-orbit(SO) coupling, known as Rashba SO interaction which arises due to structural inversion asymmetry [2].

In recent years it has been realized that SO coupling can be used to efficiently generate and detect spin-polarized current in semiconductor heterostructure without the Ferromagnetic contacts [3]. The phenomena of spin accumulation at the sample edges due to a bulk spin current transverse in direction to an applied electric field is called Spin-Hall effect(SHE) [4]. In finite size sample with SO coupling when an unpolarized charge currents passes it generates spin currents(via SO scattering) in transverse direction. This can leads to spin accumulation at the lateral edges of the sample. The experimental evidence of SHE reported in [5–7] were found by measuring the spin accumulation on the sample edges. However, such measurements are still debatable as a probe for bulk spin current since the spin accumulation can also be found even in the absence of bulk current. Apart from these, many other studies which were focused on spin accumulation due to SHE include both, the experimental [8–10] as well as the theoretical ones [11–15]. In such systems the spin accumulation and its relation to bulk spin current is a complex issue. This complexity can be understood in terms of following arguments. In a system with strong SOC, the spin-relaxation lengths are usually larger than the mean free path, spin accumulation at the edges determined by spin current coming from the bulk. In contrary to that, in the quasi-ballistic regime where the mean free path is much smaller compared to the sample size, it was shown that there is no relation between the bulk spin current and the accumulation of spins at the edges [16–18]. Considering the former case, in finite size sample, the lateral edges of the sample acts like an impenetrable barrier for particles which carries spin. Therefore the boundary spin accumulation in such systems is affected by the elastic scattering of spin polarized carriers from the sample boundary in presence of SO coupling [19]. More precisely, spin-dependent elastic reflection from an impenetrable barrier in the presence of SOC depends on the spin-orientation of particles which in-turn affects the spin accumulation [20]. Hence spin accumulation at sample boundary not only depends on the bulk spin current

[a] e-mail: shishir.kr.pandey@gmail.com
[b] *Present address*: International Center for Quantum Materials, School of Physics, Peking University, Beijing 100871, P.R. China.

but also on the spin-dependent scattering from the lateral impenetrable barrier. Spin-dependent elastic reflection of 2DEG from an impenetrable barrier in the presence of Rashba SOC was studied in references [21], where it was shown to generate spin polarized reflected beam.

The spin-orbit coupling owes its origin to appearance of inversion symmetry breaking electrical fields whether they arise intrinsically in the band structure(lack of inversion center) or by an external confining potential. In the former case inversion symmetry is broken locally and resulting SO interaction is known as Dresselhaus spin-orbit coupling [22], while in the later case confining potential leads to structure inversion asymmetry which breaks inversion symmetry globally and leads to appearance of Rashba spin-orbit coupling [2]. Thus the SHE arises from extrinsic factor like the properties of impurities can be described by a Dresselhaus like term while SHE arising from intrinsic effect related to SOC in a perfect crystal can be described by a Rashba like term.

Beside these two, another type of SOC arises due to presence of heavy impurity known as Impurity induced SOC. In low-dimensional nanosystem all these different type of SO couplings may be present simultaneously and compete with each other. Among all these Rashba SOC is more important because of its tunability via external gate voltage,while Dresselhaus and impurity induced SOC is fixed and determined by the material properties,crystal structure and impurity type and concentration respectively. Rashba and Dresselhaus SOC are also known as *intrinsic* SOC because of their origin in the band structure while impurity induced SOC is known as *extrinsic* SOC. Although both Rashba and Dresselhaus SOC are linear in momentum, however, there is an important difference, i.e., the Rashba coupling is isotropic while Dresselhaus coupling is anisotropic, i.e., depends on the orientation of crystal. This is so because the Rashba coupling is determined by globally inversion asymmetry and is independent of crystal structure while Dresselhaus crucially depends on the crystal structure as it originates due to local inversion asymmetry. The simultaneous presence of both Rashba and Dresselhaus couplings together with the tunability of Rashba SOC allows greater control over spin polarized transport [23] which in turn gives rise to many interesting and novel phenomena such as, ballistic spin field effect transistor, persistent spin helix [24] and spin edge helices [25] etc.

In view of this, we present a detailed study of spin dependent scattering of a ballistic incoming electron beam in confined geometry in presence of both Rashba an Dresselhaus SO coupling . The anisotropic nature of Dresselhaus SO coupling leads to an anisotropic Fermi energy. This anisotropy in conjugation with the tunability of Rashba coupling affects the spin dependent double refraction as well spin accumulation in a nontrivial way as we will see later. It is also shown that even if we take unpolarized incoming beam, the net polarization is coming out to be non-zero. In the over critical region all the three component of spin polarization are present and are exponentially decaying as distance from the barrier increases.

2 Model and anisotropic Fermi surface

The model Hamiltonian including both Rashba and Dresselhaus coupling has the form,

$$H_0 = \frac{\hbar^2 k^2}{2m^*} + \alpha(\sigma_x k_y - \sigma_y k_x) + \beta(\sigma_y k_y - \sigma_x k_x), \quad (1)$$

where $\mathbf{k} = (k_x, k_y, 0)$ is the 2 in-plane wave vector and m^* is effective mass. The second and third term in equation (1) are Rashba and Dresselhaus SOC with α and β as coupling coefficients respectively. The spin split eigen function and dispersion is

$$\Psi_\lambda(\mathbf{r}) = \frac{e^{\mathbf{k}\cdot\mathbf{r}}}{\sqrt{2}} \begin{pmatrix} e^{i\varphi_\rho} \\ \lambda \end{pmatrix} \quad (2)$$

$$E_\lambda(\mathbf{k}) = \frac{\hbar^2}{2m^*}\left[k^2 + \lambda\frac{2km^*}{\hbar^2}|\rho(\alpha,\beta,\phi_k)|\right]$$
$$\equiv \frac{\hbar^2}{2m^*}\left[(k + \lambda\frac{m^*}{\hbar^2}|\rho(\alpha,\beta,\phi_k)|)^2 - \frac{m^{*2}}{\hbar^4}|\rho(\alpha,\beta,\phi_k)|^2\right] \quad (3)$$

with

$$\begin{aligned}\rho(\alpha,\beta,\phi_k) &= (i\alpha e^{-i\phi_k} - \beta e^{-i\phi_k})|\rho(\alpha,\beta,\phi_k)| \\ &= \sqrt{\alpha^2 + \beta^2 - 2\alpha\beta\sin(2\phi_k)}\end{aligned} \quad (4)$$

where ϕ_k being the polar angle of in plane momentum $\mathbf{k} \equiv (k\cos\phi_k, k\sin\phi_k)$. The spinor phase is given by $\varphi_\rho = Arg[\rho(\alpha,\beta,\phi_k)]$ and $\lambda = \pm 1$ defines the chirality of the eigenfunctions. The Fermi wave vectors for a fixed energy(E_F) are

$$k_\lambda = \frac{1}{\mu}\left(\sqrt{2\mu E_F + |\rho|^2} - \lambda\rho\right) \quad (5)$$

where $E_F = E_+(k_+) = E_-(k_-)$.

The spin split dispersion given by equation (3) is shown in Figure 1 for various values of α and β In the dispersion curves shown above, the first corresponds (panel a) to the simple Rashba system ($\beta = 0$) and the rest three figures corresponds to the three different cases, namely for $\alpha = \beta$, $\alpha > \beta$, $\alpha < \beta$ respectively. The qualitative plot shows the asymmetric Fermi energy surfaces in the k_x–k_y plane. Note that when $\alpha = \beta$ (Fig. 1b) the curves touch each other along particular direction in k-space. This implies that for waves propagating along this direction spin splitting vanishes, and as a consequence precession induced spin dephasing ceases to act. This property was used in the non-ballistic spin field effect transistor proposed by Schliemann et al. [26]. For $\alpha \neq \beta$ (Figs. 1c and 1d), the two Fermi surface becomes anisotropic in k_x–k_y plane. Therefore simultaneous presence of both Rashba and Dresselhaus spin orbit coupling provides a much better control over the spin splitting and we will see later that this leads to interesting phenomena for spin dependent elastic reflection from impenetrable barriers.

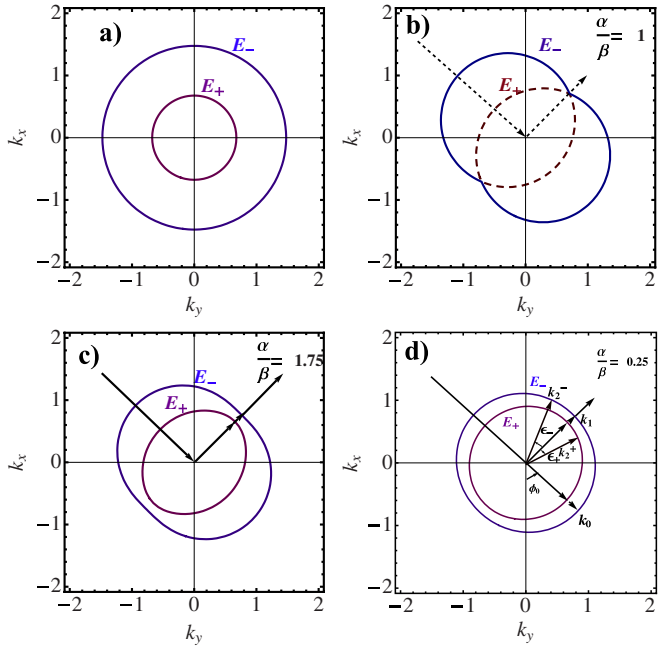


Fig. 1. (a–d) Illustrating the dispersion curves for various values of α and β. (a) Corresponds to $\alpha = 1$ and $\beta = 0.0$, for remaining (b–d) these parameters are shown in the figure itself. The two circles shows the constant energy contours in (k_x, k_y) plane for the two chiral branches E_λ. Depending upon relative magnitude α/β, these circles can cross each other (b) or become anisotropic as in (c).

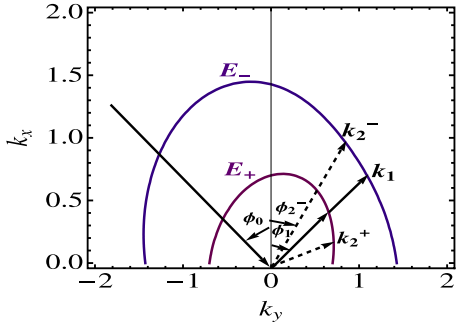


Fig. 2. Figure showing the ordinary and extra-ordinary reflection. The solid lines correspond to ordinary reflected wave while dashed lines are used to show the extra-ordinary reflection. Here $\alpha/\beta = 0.25$.

2.1 Elastic spin dependent scattering from impenetrable barrier

We consider two dimensional system in xy plane with an impenetrable barrier $V(x)$ along $\hat{x}$ axis,which is described by the Hamiltonian,

$$H = H_0 + V(x), \tag{6}$$

where H_0 is defined in equation (1). We assume that $V(x) = 0$ for $x < 0$ and $V(x) = \infty$ for $x > 0$ and along $\hat{y}$ axis systems is free. Consider an electron beam with chirality λ and wave vector k_0^λ incident on impenetrable barrier at an angle ϕ_0. It is reflected elastically from the barrier and due to splitting of dispersion curves this processes generates two reflected waves, namely, ordinary reflected wave and extraordinary reflected wave. For ordinary reflection, energy as well momentum both are conserved while for extraordinary wave only energy is conserved. This is shown schematically in Figure 2. The wave vectors for incident, ordinarily(momentum preserving) and extraordinary reflected waves are with k_{in}^λ, k_1^λ and $k_2^{-\lambda}$ respectively. The most general scattering wave function for this system is the linear combination of these three and can be written as,following reference [21],

$$\begin{aligned}\psi_k^\lambda(r) = &\frac{\exp^{ik_0^\lambda.r}}{\sqrt{2A}\rho}\begin{pmatrix} i\alpha e^{-i\phi_0} - \beta e^{i\phi_0} \\ \lambda\rho \end{pmatrix} \\ &+ \frac{A_1^\lambda \exp^{ik_1^\lambda.r}}{\sqrt{2A}\rho}\begin{pmatrix} i\alpha e^{-i\phi_1^\lambda} - \beta e^{i\phi_1^\lambda} \\ \lambda\rho \end{pmatrix} \\ &+ \frac{A_2^{-\lambda} \exp^{ik_2^{-\lambda}.r}}{\sqrt{2A}\rho}\begin{pmatrix} i\alpha e^{-i\phi_2^{-\lambda}} - \beta e^{i\phi_2^{-\lambda}} \\ -\lambda\rho \end{pmatrix}.\end{aligned}$$

Translational invariance parallel to the barrier at $x = 0$ implies that y-component of crystal momentum is conserved, hence,

$$k_y = k_0^\lambda \sin\phi_0 = k_1^\lambda \sin\phi_1 = k_2^{-\lambda} \sin\phi_2^{-\lambda} \tag{7}$$

from which one obtains the angle of reflection for ordinary (ϕ_1) and extraordinary beams (ϕ_2) as,

$$\phi_1 = \pi - \phi_0 \tag{8}$$

$$\phi_2^{-\lambda} = \pi - \arcsin\left(\frac{k_{+\lambda}}{k_{-\lambda}} \sin\phi_0\right). \tag{9}$$

In general ϕ_1 and ϕ_2 are different, implying that a single incident wave with a particularly chirality generate waves of both chirality as is shown in Figure 2. The ordinary reflected wave is always propagating while the extraordinary wave may be propagating or evanescent depending on whether $\phi_2^{-\lambda}$ is real or imaginary. Since $k_- > k_+$, ϕ_2^- has always a real value for $0 \le \phi_0 \le \frac{\pi}{2}$ but in case of ϕ_2^+ a real solution exits only for ϕ_c after which this angle becomes complex, where

$$\phi_c = \arcsin\left(\frac{k_+}{k_-}\right). \tag{10}$$

The splitting angle i.e. the angular difference between the two reflected beam is

$$\epsilon_{-\lambda} \equiv \phi_0 - \arcsin\left(\frac{\sqrt{2\mu E + |\rho|^2} - \lambda\rho}{\sqrt{2\mu E + |\rho|^2} + \lambda\rho} \sin\phi_0\right). \tag{11}$$

The angle ϵ_- and ϵ_- have their largest value given by

$$|\epsilon_{\max}| = \frac{\pi}{2} - \phi_c \tag{12}$$

obtained at $\frac{\pi}{2}$ and ϕ_c respectively. The splitting angle ϵ_- is positive while ϵ_+ is negative From the conservation of k_y^λ, it can be seen that the k_{x1}^λ and $k_{x2}^{-\lambda}$ become functions of ϕ_1 and $\phi_2^{-\lambda}$ respectively. When $\phi_0 > \phi_c$, k_2^+ becomes imaginary and leads to exponentially decaying current. At the interface, the wave function must be continuous which yields the conditions

$$A_1^\lambda = \left(\frac{e^{-2i\phi_0} - e^{-i\epsilon_{-\lambda}}}{1 + e^{-i\epsilon_{-\lambda}}}\right)\left\{\frac{i\alpha e^{-i\epsilon_{-\lambda}} + \beta}{i\alpha e^{-i\epsilon_{-\lambda}} - \beta e^{-2i\phi_0}}\right\} \quad (13)$$

$$A_2^{-\lambda} = \left(\frac{1 + e^{-2i\phi_0}}{1 + e^{-i\epsilon_{-\lambda}}}\right)\left\{\frac{i\alpha e^{2i\phi_0} - \beta e^{2i\phi_0}}{i\alpha e^{2i\phi_0} - \beta e^{i\epsilon_{-\lambda}}}\right\}. \quad (14)$$

Using the above equation it is straight forward to obtain ordinary ($R_{\lambda\lambda} = \frac{A_1^\lambda}{A_0}$) and extraordinary ($R_{\lambda-\lambda} = \frac{A_1^\lambda}{A_0}$) reflection coefficients,

$$R_{\lambda\lambda} = \left(\frac{\sin^2\left(\frac{\epsilon_{-\lambda}}{2} - \phi_0\right)}{\cos^2\frac{\epsilon_{-\lambda}}{2}}\right) \times \left\{\frac{\alpha^2 + \beta^2 + 2\alpha\beta\sin\epsilon_{-\lambda}}{\alpha^2 + \beta^2 - 2\alpha\beta\sin\left(\epsilon_{-\lambda} - 2\phi_0\right)}\right\} \quad (15)$$

$$R_{\lambda-\lambda} = \left(\frac{\cos^2\phi_0}{\cos^2\frac{\epsilon_{-\lambda}}{2}}\right)\left\{\frac{\alpha^2 + \beta^2}{\alpha^2 + \beta^2 - 2\alpha\beta\sin\left(\epsilon_{-\lambda} - 2\phi_0\right)}\right\}. \quad (16)$$

In the above expressions (13)–(16), the terms in curly brackets reduces to one for $\beta = 0$ which agrees with the previous result of reference [21]. In general the dependence on α, β is more complicated as is clear from the above expressions. To obtain insight and compare it with the simple Rashba system we plot reflection coefficient as a function of incident angles in Figure 3 for the three different cases i.e. $\alpha > \beta$, $\alpha < \beta$, $\alpha = \beta$. From Figure 3 we notice that when the strength of Rashba and Dresselhaus SOC are different, the four reflection coefficients are never equal at any incident angle. This is consistent with the anisotropic Fermi contours in Figures 1c and 1d. For $\alpha = \beta$ at 45° all four reflection coefficients become equal since at this point the two Fermi contours cross each other. The is again reflected in the splitting angle which is plotted in Figure 4, again the splitting vanishes for $\alpha = \beta$ at 45° and for all other cases it never vanishes. We stress that this vanishing of splitting angle or crossing of Fermi contours happens only if both Rashba and Dresselhaus couplings are present and of equal strength. If only Rashba or only Dressehaus coupling is present then this will not be the case. This implies that at a particular angle of incident the reflection from impenetrable barrier would not produce spin polarization only for $\alpha = \beta$ case and in this atypical case only the boundary spin accumulation will be fully determined by the bulk spin currents. However in quasi one dimensional systems (finite transverse width) since the electrons will be approaching boundary from all possible incident angles, therefore the boundary spin accumulation in general will be determined by both bulk spin current as well by the reflection from the boundary.

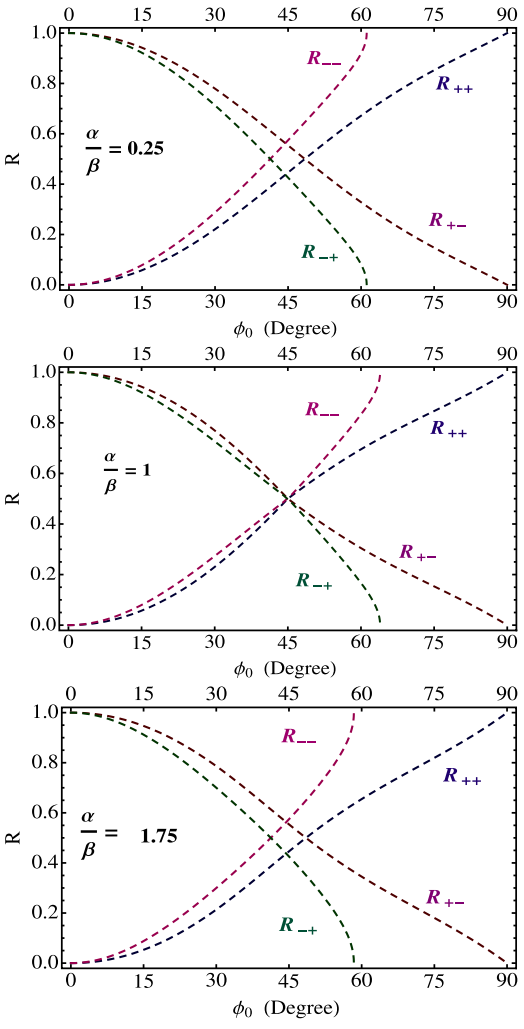


Fig. 3. Reflection coefficient $R_{\lambda\lambda}$ for the three different ($\alpha > \beta$, $\alpha = \beta$, $\alpha < \beta$) cases for R and D system as a function of incident angle is shown.

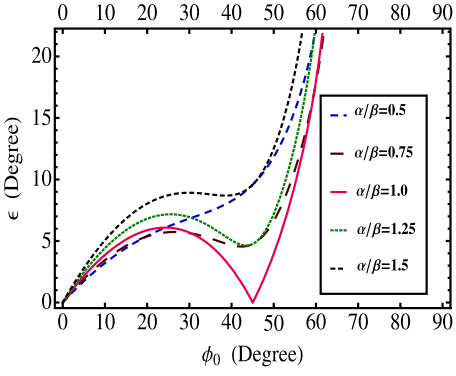


Fig. 4. Total splitting angle as a function of incident angle is shown. It is shown that at 45° when $\alpha = \beta$, then the polarization is completely vanishes.

3 Velocity and current

We calculate the expression for the velocity Operator from the Hamiltonian (1) and is given by:

$$\mathbf{v} = \frac{1}{\hbar}\left[\mu k + \alpha\left(\hat{j}\sigma_x - \hat{i}\sigma_y\right) - \beta\left(\hat{i}\sigma_x - \hat{j}\sigma_y\right)\right]. \quad (17)$$

While considering the real angles ϕ the magnitude v of the velocity:

$$v \equiv \langle v\rangle = \frac{1}{\hbar}\left[\mu k_\lambda + \lambda\left(\alpha - \beta\right)\right]. \quad (18)$$

We see here that for real angles the velocity is same for all the beams but the velocity will be slightly higher for the complex angle ϕ_2^+. We do not here give the lengthy expression. Also the probability current calculation gives:

$$\mathbf{j} \equiv \langle j\rangle = \frac{i}{\hbar}\left[\mu\mathbf{Re}\left(\langle\psi|k|\psi\rangle\right) + \alpha\left(\left\langle\psi|\hat{j}\sigma_x - \hat{i}\sigma_y|\psi\right\rangle\right)\right] - \frac{i}{\hbar}\left[\beta\left(\left\langle\psi|\hat{i}\sigma_x - \hat{j}\sigma_y|\psi\right\rangle\right)\right]. \quad (19)$$

As expected, $j_x = 0$ for an impenetrable barrier in both the cases of incoming and reflected beam while j_y, for the region in which both the components of beam are present, oscillates as a function of distance from the barrier. It can be realized by considering the interference terms of the three components of the wave function. For the real angles, we get

$$J_0^\lambda = |A_0|^2 v_0 \quad (20)$$

$$J_1^\lambda = |A_0|^2\left(\frac{\sin^2\left(\frac{\epsilon_{-\lambda}}{2} - \phi_0\right)}{\cos^2\frac{\epsilon_{-\lambda}}{2}}\right) \times\left(\frac{\alpha^2+\beta^2+2\alpha\beta\sin\epsilon_{-\lambda}}{\alpha^2+\beta^2-2\alpha\beta\sin\left(\epsilon_{-\lambda}-2\phi_0\right)}\right) v_1 \quad (21)$$

$$J_2^{-\lambda} = |A_0|^2\left(\frac{\cos^2\phi_0}{\cos^2\frac{\epsilon_{-\lambda}}{2}}\right) \times\left(\frac{\alpha^2+\beta^2}{\alpha^2+\beta^2-2\alpha\beta\sin\left(\epsilon_{-\lambda}-2\phi_0\right)}\right) v_2^{-\lambda}. \quad (22)$$

In over-critical region i.e. for the complex angle ϕ_2^+:

$$J_2^+ = |A_0|^2\left(\frac{2\cos^2\phi_0}{\cos\epsilon_{\max}}\right) \times\left(\frac{\alpha^2+\beta^2}{\alpha^2+\beta^2-2\alpha\beta\sin\left(\epsilon_{-\lambda}-2\phi_0\right)}\right) \times e^{2k_2^+ x} v_2^+ \quad (23)$$

the current decays exponentially as the distance $|x|$ increases from the barrier.

Figure 5 shows the net polarization (which is the addition of polarization of ordinary and extra-ordinary reflected beams) at different Rashba and Dresselhaus SOC strength, against the incident angle. The plot at different SOC strength is shown from which it is clear that net

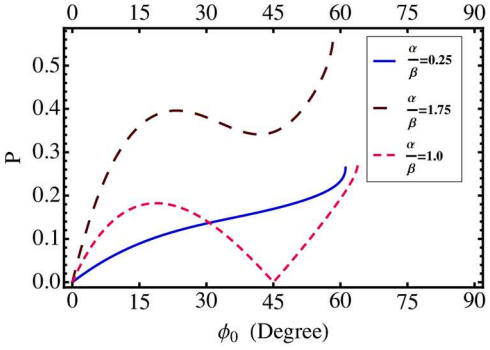


Fig. 5. Plot shows the net polarization of reflected beams against the incident angle at different values of α and β. Here interference terms are absent.

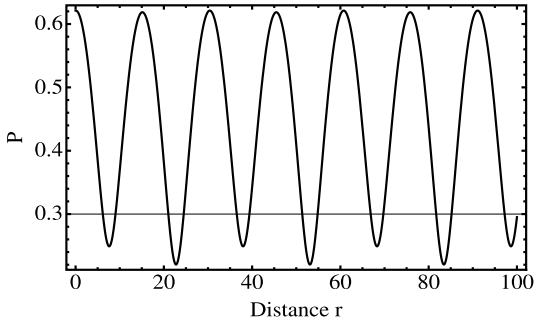


Fig. 6. Plot for the net polarization of the beam incident at the angle $\frac{\pi}{3}$. Here the interference terms are taken into consideration.

Polarization is non-zero at all the values of incident angle except at 45°.

We calculate the net polarization which is plotted against the distance r from the barrier which is shown in Figure 6. In this plot, value of Rashba SOC strength α is taken to be equal to the Dresselhaus SOC strength β. The contribution to this polarization is because of the two terms. In the first is term we have individually calculated and then added up the polarization for the incident, ordinarily and extraordinarily reflected beam. In the second term, polarization is calculated for the interference terms of these three components of the beam.The value of net polarization is always non-zero at all the values of the incident angle except at 45° and oscillates with two different frequencies.

In Figure 7, for the over-critical region it is clearly shown that all the three components of polarization of extraordinary reflected beam will be present irrespective of the three cases of SOC strengths i.e. $\alpha < \beta$, $\alpha > \beta$ and $\alpha = \beta$. Also in this region the net polarization always has non-zero values. All the three components of polarization as well as the net polarization will exponentially decay as the distance from the barrier increases. This is shown in Figure 8.

This non-propagating non-zero polarization gives rise to spin-accumulation near the barrier which is clearly an important consequence of spin-dependent elastic reflection from a impenetrable barrier in the presence of R and D

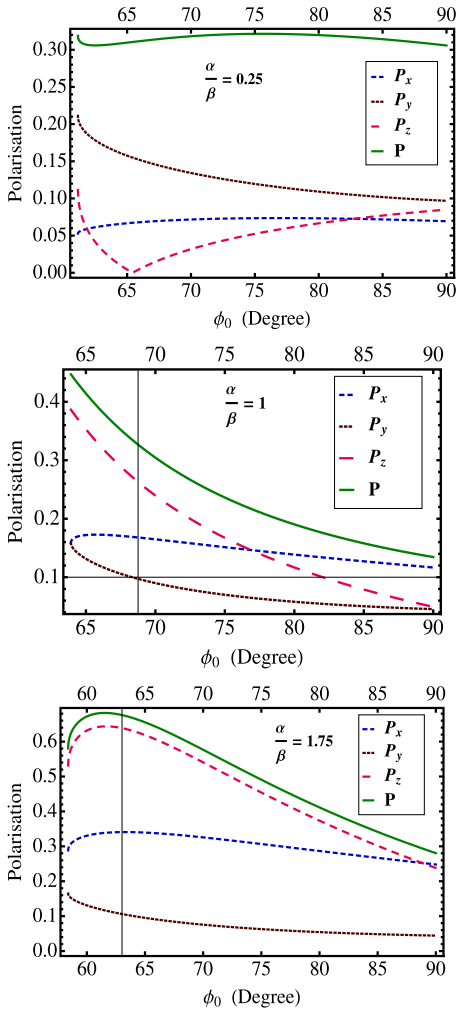


Fig. 7. Different components of polarization with non-zero net polarization of extraordinary reflected beam in over critical region is plotted against incident angle ϕ_0 for the different values of α and β. P_x, P_y, P_z are the x, y and z component of polarization. P is the net polarization.

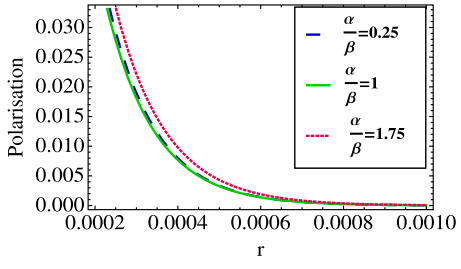


Fig. 8. Plot for the net polarization of the non-propagating component in the over critical region for the three different cases of α and β. Here the angle of incidence is 75° and $r = \frac{r_0}{d}$ is the SOC range where $d = 5\times10^{-4}$ unit.

SOC. So it is clear that spin-accumulation near the barrier is a typical phenomena in which spin-accumulation near the barrier will not only depend upon the bulk spin-current but also on the spin-dependent scattering from the lateral impenetrable barrier which can be think of the lateral edges of the sample.

4 Conclusion

In conclusion, present work shows that the spin-orientation of the electrons changes because of the spin-dependent reflection from an impenetrable barrier in the presence Rashba and Dresselhaus SOC. It gives rise to a new mechanism of multiple reflection analogous to the birefringence phenomena. Also an important feature of anisotropy in the Fermi energy surface come into appearance because of this reflection. We also observed that increase in the value of Dresselhaus SOC strength β gives increases the anisotropy in the system. In this case a non-zero spin-polarized current is observed for all incident angle between 0 and $\frac{\pi}{2}$ except at angle of 45° which is clearly an another important feature of Rashba and Dresselhaus SOC interplay. Also it is shown that in the over-critical region,there is some spin-accumulation near the barrier is also affected by scattering of the bulk spin-current from the lateral edges of the sample which in turns affect the spin-accumulation as in the case of spin-hall effect.

S.K. Pandey would like to acknowledge Dr. Rajarshi Tiwari, Dr. Ram Lal Awasthi and Dr. Vikas Chauhan for their academic support and discussions.

Author contribution statement

SKP has worked on the idea with the help of TPP. SKP has written the manuscript which was further improved by TPP.

References

1. S. Datta, B. Das, Appl. Phys. Lett. **56**, 665 (1990)
2. Y.A. Bychkov, E.I. Rashba, J. Phys. C **17**, 6039 (1984)
3. T.P. Pareek, Phys. Rev. Lett. **92**, 076601 (2004)
4. M.I. D′yakonov, V.I. Perel, J. Exp. Theor. Phys. Lett. **13**, 467 (1971)
5. V. Sih, R.C. Myers, Y.K. Kato, W.H. Lau, A.C. Gossard, D.D. Awschalom, Nat. Phys. **1**, 31 (2005)
6. J. Wunderlich, B. Kaestner, J. Sinova, T. Jungwirth, Phys. Rev. Lett. **94**, 047204 (2005)
7. Y.K. Kato, R.C. Myers, A.C. Gossard, D.D. Awschalom, Science **306**, 1910 (2004)
8. V. Sih, W.H. Lau, R.C. Myers, V.R. Horowitz, A.C. Gossard, D.D. Awschalom, Phys. Rev. Lett. **97**, 096605 (2006)
9. N.P. Stern, D.W. Steuerman, S. Mack, A.C. Gossard, D.D. Awschalom, Appl. Phys. Lett. **91**, 062109 (2007)
10. B. Kaestner, J. Wunderlich, T. Jungwirth, J. Sinova, K. Nomura, A.H. MacDonald, Physica E **34**, 47 (2006)
11. M.I. Dyakonov, V.I. Perel, Phys. Lett. A **35**, 459 (1971)
12. J.E. Hirsch, Phys. Rev. Lett. **83**, 1834 (1999)
13. S. Zhang, Phys. Rev. Lett. **85**, 393 (2000)
14. S. Murakami, N. Nagaosa, S.-C. Zhang, Science **301**, 1348 (2003)

15. J. Sinova, D. Culcer, Q. Niu, N.A. Sinitsyn, T. Jungwirth, A.H. MacDonald, Phys. Rev. Lett. **92**, 126603 (2004)
16. A. Khaetskii, E. Sukhorukov, Phys. Rev. B **87**, 075303 (2013)
17. A. Khaetskii, Phys. Rev. B **89**, 195408 (2014)
18. A. Khaetskii, J. Carlos Egues, Europhys. Lett. **118**, 57006 (2017)
19. H. Chen, J.J. Heremans, J.A. Peters, A.O. Govorov, N. Goel, S.J. Chung, M.B. Santos, Appl. Phys. Lett. **86**, 032113 (2005)
20. G. Usaj, C.A. Balseiro, Europhys. Lett. **72**, 631 (2005)
21. V. Teodorescu, R. Winkler, Phys. Rev. B **80**, 041311 (2009)
22. G. Dresselhaus, Phys. Rev. **100**, 580 (1955)
23. R. Winkler, *Spin-Orbit Coupling Effects in Two-Dimensional Electron and Hole Systems* (Springer, Berlin, 2003)
24. J.D. Koralek, C. Weber, J. Orenstein, A. Bernevig, S.-C. Zhang, S. Mack, D. Awschalom, Nature **458**, 610 (2009)
25. S.M. Badalyan, J. Fabian, Phys. Rev. Lett. **105**, 186601 (2010)
26. J. Schliemann, J. Carlos Egues, D. Loss, Phys. Rev. Lett. **90**, 146801 (2003)